

Faceting of Nanocrystals during Chemical Transformation: From Solid Silver Spheres to Hollow Gold Octahedra

Yadong Yin,^{†,‡,||} Can Erdonmez,^{‡,§} Shaul Aloni,^{†,‡} and A. Paul Alivisatos^{*,†,‡,§}

The Molecular Foundry and Materials Science Division at the Lawrence Berkeley National Laboratory, Berkeley, California 94720, and Department of Chemistry, University of California at Berkeley, Berkeley, California 94720

Received June 29, 2006; E-mail: alivis@berkeley.edu

Sustained progress in nanocrystal synthesis has enabled recent use of these materials as inorganic, macromolecular precursors that can be chemically transformed into new nanostructures.¹ The literature now contains several cases with chemical transformations being accompanied by varying degrees of modification of properties, including crystal structure and particle shape.² As a recent example, we demonstrated that as-synthesized metallic nanocrystals yield, upon oxidation, nanostructures with modified morphologies such as hollow particles.³ The morphological change derives, in this case, from directional material flows due to differing diffusivities for the reacting atomic species, in a nanoscale version of the well-known Kirkendall Effect. The methodology has since been demonstrated by others to yield nanostructures with various compositions and shapes.⁴

Galvanic replacement reactions have been shown to also produce hollow nanostructures. Xia et al. reported cases where a replacement reaction took place uniformly around Ag cubes of ~100 nm size, leading to formation of Au nanoboxes.⁵ The exterior shape of the nanoboxes tends to largely reproduce that of the sacrificial Ag counterparts. Here, we report that performing the same replacement reaction on silver nanocrystals that are an order of magnitude smaller leads to significant changes in the external morphology of the Au shells as the reaction proceeds, while still creating a central void in each particle. Specifically, single crystalline silver nanocrystals with a spherical shape act in the presence of Au³⁺ as precursors for formation of hollow Au nanocrystals with truncated octahedral shape. The growth of significantly faceted particles from spherical precursors is made possible by surface effects, namely surfactant binding and/or an enhanced role for surface energetics in our smaller nanocrystals. Production of hollow Au nanocrystals with faceted geometry allows increased tunability of optical properties as the surface plasmon resonance of a hollow metallic nanocrystal depends strongly not only on the shell thickness, but also on the detailed shape.⁶

To produce Ag nanocrystals with reduced sizes and improved monodispersity, we performed the synthesis using a modification of the polyol process in an organic solvent and at high temperature.^{3,7} The silver salt AgNO₃ was reduced by 1,2-hexadecanediol in an organic solvent, *o*-dichlorobenzene (DCB). Oleylamine was present as a surfactant. Rapid formation of silver nanocrystals upon reaction was indicated by the originally colorless solution turning dark brown. The transformation of solid nanocrystals into hollow ones was performed through galvanic replacement by dropwise addition of AuCl₃ solution to diluted silver colloidal solution until the solution changed in color from dark yellow to blue. In this

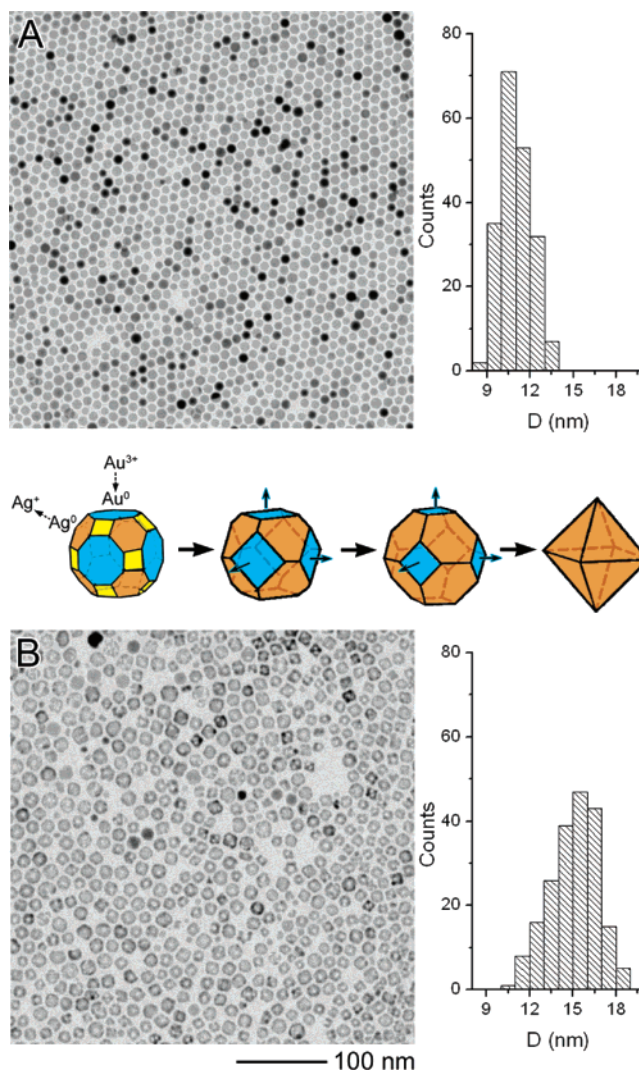


Figure 1. (A) TEM image of silver nanocrystals and the measured particle diameter distribution. (B) TEM image and diameter distribution for gold hollow nanocrystals obtained by performing a replacement reaction on the silver nanocrystals in image A. The schematic illustration between images A and B shows the proposed mechanism for the formation of gold truncated octahedra. A truncated cuboctahedron is used to represent the starting spherical silver nanocrystal. A replacement reaction between gold and silver removes silver atoms preferentially from (111) facets, while depositing gold atoms selectively to higher energy facets such as (100) and (110).

reaction, oleylamine likely serves two purposes. First, it solubilizes the precursors AgNO₃ and AuCl₃ in DCB. Second, it acts as a surfactant that controls the growth of nanocrystals and stabilizes the colloidal solution.

[†] Molecular Foundry, Lawrence Berkeley National Laboratory.

[‡] Materials Science Division, Lawrence Berkeley National Laboratory.

[§] University of California at Berkeley.

^{||} Current address: Department of Chemistry, University of California at Riverside, Riverside, CA 92521. E-mail: yadong.yin@ucr.edu.

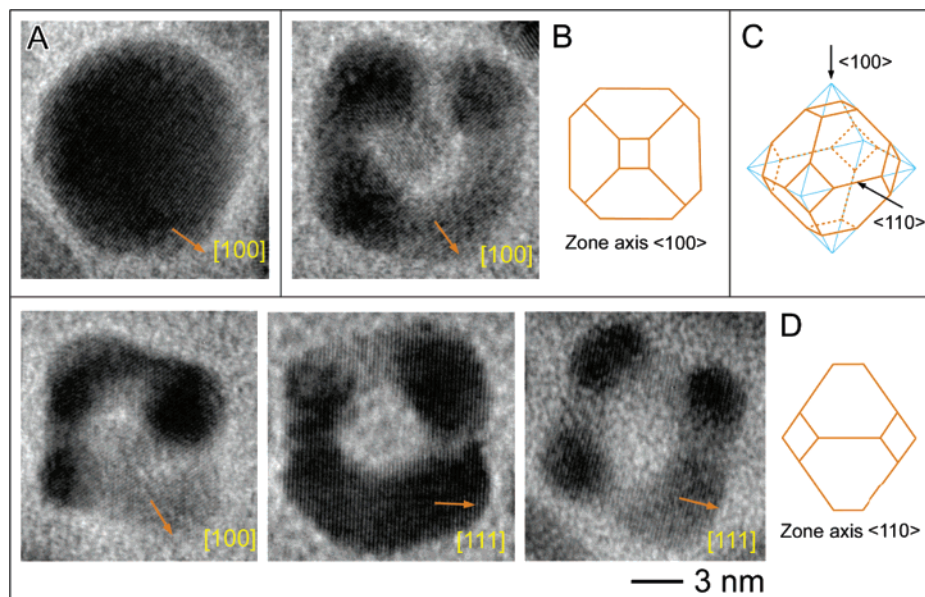


Figure 2. (A) HRTEM image of a silver nanocrystal, confirming spherical morphology and single crystalline structure. (B–D) HRTEM images of gold hollow nanocrystals, showing a faceted morphology and a single crystalline domain within each particle: (B) imaged along the $\langle 100 \rangle$ direction and (D) imaged along the $\langle 110 \rangle$ direction. Various views of the faceted nanocrystals are consistent with a truncated octahedron as the dominant particle shape, as illustrated schematically.

The choice of DCB as the solvent allows us to synthesize silver nanocrystals at relatively high temperatures (~ 180 °C). The resulting high nucleation and growth rates make “kinetic size focusing” possible, favoring formation of monodisperse nanocrystals.^{1,8} Indeed, as-synthesized silver nanocrystals have narrow size distributions, as seen in the transmission electron microscopy (TEM) image and the observed particle diameter statistics for a typical sample (Figure 1A). All the nanocrystals possess an apparently spherical shape, and the average diameter is 11.0 ± 1.1 nm. Nanoparticle size can be tuned by varying reaction conditions such as the growth duration, temperature, and the molar ratio between the surfactant and silver precursor.⁹ We also notice that the nanocrystals synthesized in this case have average sizes much smaller than those produced using the regular polyol process which typically uses ethylene glycol as solvent as well as reducing agent, and poly(vinylpyrrolidone) (PVP) as surfactant.¹⁰ This suggests stronger attachment of oleylamine than PVP to the silver nanocrystal surface.

Performing a replacement reaction on Ag nanocrystals with dissolved Au^{3+} at 45 °C leads to formation of hollow gold nanocrystals with slightly broadened size distribution, as shown in Figure 1B. Contrast is sensitive to mass-thickness in conventional TEM images; consequently, hollow particles appear lighter at their center in images. Energy dispersive X-ray analysis (EDX) on Au hollow nanocrystals typically does not give rise to a well-resolvable Ag signal, implying that the replacement reaction proceeds essentially to completion and that Ag is present at $<5\%$, if at all, in these nanocrystals (Supporting Information).

Inspection of the hollow nanocrystals reveals that they have faceted morphology instead of the spherical shape of the original Ag particles, with many of them clearly presenting a rhomboid outline. As the faceted nanocrystals are viewed along various projections in TEM images, the size dispersion of the sample is difficult to characterize exactly. Measuring the longest dimension observed in images of individual hollow crystals yields an average length of 15.1 ± 1.7 nm, a number significantly larger than that of the starting Ag particles. The increase in length cannot be attributed to systematic errors during size measurements; instead, it indicates

that the particles grow outward along certain directions during the replacement reaction.

Figure 2A shows the high-resolution TEM (HRTEM) image of a Ag nanocrystal before the replacement reaction. Lattice fringes are separated by 2.04 Å corresponding to $\{200\}$ planes of face-centered cubic Ag. Unlike the regular polyol process where Ag nanocrystals usually contain defects such as multiple twins,^{5,11} our modified method produces only single crystalline spherical Ag particles. The hollow nanocrystals obtained by the replacement reaction retain the single crystalline structure despite significant shape change. The various profiles observed in images of hollow nanocrystals can be shown to correspond to various projections of a truncated octahedron enclosed by six $\{100\}$ and eight $\{111\}$ facets (Figure 2C).¹² Parts B and D of Figure 2 show HRTEM images and schematic illustrations of how viewing of nanocrystals along particular directions accounts for the different images. When a nanocrystal lies on a $\{100\}$ facet, the projected image is a square with four corners slightly cut off (Figure 2B). The observed orientation of $\{200\}$ fringes parallel to square diagonals is expected in this case. Figure 2D shows the case when a nanocrystal sits on one of its edges between two $\{111\}$ facets. The projection is now along $\langle 110 \rangle$ and the particle presents a rhomboid shape with two corners cut off. HRTEM images display lattice fringes with a spacing corresponding either to $\{200\}$ or $\{111\}$ planes, depending on imaging conditions. On the basis of these observations, we conclude that the spherical Ag nanocrystals have been transformed into hollow, truncated octahedra. The degree of truncation varies from particle to particle; typically, the size of a corner facet is small in comparison to the edge length of the octahedron.

The shape transformation from Ag nanospheres to Au truncated octahedra involves a number of processes including the oxidation and dissolution of Ag atoms, reduction and deposition of Au atoms, and counterdiffusion of vacancies and atoms. It is not yet possible to detail an exact mechanism, but some general observations may be made about the formation process. The trend typically observed for surface energies of the low-index faces for noble metal crystals is $\gamma_{111} < \gamma_{100} < \gamma_{110}$.¹¹ For our Ag synthesis conditions, the apparently spherical shape of the resulting particles indicates that

several different families of slow-growing facets grow at a similar rate. When silver nanocrystals are subjected to the replacement reaction, the Au^{3+} cations are reduced and deposited on the surface of Ag nanocrystals. Net growth or etching of each facet during the reaction is determined by the competition between Au atom deposition and Ag atom dissolution occurring at that facet. Our results are consistent with Au deposition occurring preferentially onto the high energy $\{100\}$ and $\{110\}$ facets. In an idealized picture, release of three Ag atoms from the nanocrystal for each Au atom deposited injects vacancies at the core–shell interface. Similar to the case of sulfidation of cobalt nanocrystals, a large fraction of these vacancies coalesce, producing a well-defined void in the center of each nanocrystal.³ In previous studies, pinholes were observed to form in the Au shells at later stages of the replacement reaction.¹⁰ We also observe pinholes, and they appear preferentially on $\{111\}$ facets of the hollow particles (Supporting Information), consistent with the argument that Au deposition is not preferred on these facets during the replacement reaction.

Evolution of nanocrystal shape toward an octahedral geometry during the replacement reaction is very visible in comparison to the results by Xia et al. Effectively, the *net* growth rate on $\{100\}$ faces exceeds significantly *net* growth rate on $\{111\}$ faces for our smaller, spherical nanocrystals; surprisingly, this is not the case for the 100 nm nanoboxes, where slight faceting of cube corners becomes visible only very close to completion of the reaction. Apparently, differences in growth and/or etching rate among various crystal facets are enhanced in our system. Whether this enhancement is due to the particular chemistry we employed (e.g., due to strong surfactant binding), or to size-dependent surface energies of facets cannot be specified at this point.

Consistent with previous studies, the surface plasmon peak is dramatically red shifted for hollow nanocrystals in comparison to solid counterparts (Supporting Information), owing to strong electromagnetic coupling between inner and outer surfaces of the hollow particles.⁶ As the replacement reaction proceeds, the Ag nanocrystals progressively turn from yellow to brownish yellow, greenish yellow, and eventually blue. The plasmon peak shifts to longer wavelengths because of void size increasing and a shell being formed during the replacement reaction. While the direction of the peak shift and its origin are the same for faceted hollow nanocrystals as for spherical or cubic shells, the faceted surface introduces additional parameters that may influence optical properties. Currently, we are performing spectroscopic studies on single particles to identify how surface plasmon resonance properties depend on the combined presence of central voids and a variable degree of faceting for the hollow shells.

Tu and Gösele have noted that a hollow nanocrystal is not thermodynamically stable and evolves into a solid particle with lowered surface energy through a diffusional process.¹³ On the basis of the expressions they presented, a Au shell surrounding a 4 nm

void should remain hollow for decades if the temperature is held below 150 °C. However, the pinholes observed in our structures allow for surface diffusion to operate in parallel to bulk diffusion through the shells, and should accelerate conversion of hollow structures into solid ones.

In summary, we have demonstrated that a replacement reaction performed on single crystalline silver nanospheres in an organic solvent produces hollow gold nanocrystals with faceted shape, while preserving the single crystalline nature of the starting particles. This study reveals that surface-mediated shape control and achievement of a hollow morphology can be combined in a one-pot, single-step procedure, leading to finer tuning of particle morphology. As various phenomena of deposition, etching and diffusion are coupled within the synthetic process, detailed mechanistic studies should facilitate progress along this direction.

Acknowledgment. This work was performed at the Molecular Foundry, Materials Science Division, Lawrence Berkeley National Laboratory, and was supported by the Office of Science, Office of Basic Energy Sciences, of the U.S. Department of Energy under Contract No. DE-AC02-05CH11231.

Supporting Information Available: Experimental procedures, additional HRTEM analysis, and EDX and UV–vis measurements. This material is available free of charge via the Internet at <http://pubs.acs.org>.

References

- (1) (a) Yin, Y.; Alivisatos, A. P. *Nature* **2005**, *437*, 664–670. (b) Stellacci, F. *Nat. Mater.* **2005**, *4*, 113–114.
- (2) (a) Harris, P. J. F. *Nature* **1986**, *323*, 792–794. (b) Son, D. H.; Hughes, S. M.; Yin, Y.; Alivisatos, A. P. *Science* **2004**, *306*, 1009–1012. (c) Mokari, T.; Rothenberg, E.; Popov, I.; Costi, R.; Banin, U. *Science* **2004**, *304*, 1787–1790.
- (3) Yin, Y.; Rioux, R. M.; Erdonmez, C. K.; Hughes, S.; Somorjai, G. A.; Alivisatos, A. P. *Science* **2004**, *304*, 711–714.
- (4) (a) Chang, Y.; Teo, J. J.; Zeng, H. C. *Langmuir* **2005**, *21*, 1074–1079. (b) Liu, B.; Zeng, H. C. *J. Am. Chem. Soc.* **2004**, *126*, 16744–16746. (c) Wang, C. M.; Baer, D. R.; Thomas, L. E.; Amonette, J. E.; Anthony, J.; Qiang, Y.; Duscher, G. *J. Appl. Phys.* **2005**, *98*, 094308. (d) Li, Q.; Penner, R. M. *Nano Lett.* **2005**, *5*, 1720–1725.
- (5) (a) Sun, Y.; Mayers, B. T.; Xia, Y. *Nano Lett.* **2002**, *2*, 481–485. (b) Sun, Y.; Xia, Y. *Science* **2002**, *298*, 2176–2179. (c) Selvakannan, P.; Sastry, M. *Chem. Commun.* **2005**, 1684–1686.
- (6) (a) Halas, N. *MRS Bull.* **2005**, *30*, 362–367. (b) Haes, A. J.; Haynes, C. L.; McFarland, A. D.; Schatz, G. C.; Van Duyne, R. P.; Zou, S. *MRS Bull.* **2005**, *30*, 368–375.
- (7) Sobal, N. S.; Ebels, U.; Möhwald, H.; Giersig, M. *J. Phys. Chem. B* **2003**, *107*, 7351–7354.
- (8) Peng, X.; Wickham, J.; Alivisatos, A. P. *J. Am. Chem. Soc.* **1998**, *120*, 5343–5344.
- (9) Lin, X. Z.; Teng, X.; Yang, H. *Langmuir* **2003**, *19*, 10081–10085.
- (10) (a) Fievet, F.; Lagier, J. P.; Figlarz, M. *MRS Bull.* **1989**, *14*, 29–34. (b) Sun, Y.; Xia, Y. *Nano Lett.* **2003**, *3*, 1569–1572.
- (11) Wang, Z. L. *J. Phys. Chem. B* **2000**, *104*, 1153–1175.
- (12) Harfenist, S. A.; Wang, Z. L.; Alvarez, M. M.; Vezmar, I.; Whetten, R. L. *J. Phys. Chem.* **1996**, *100*, 13904–13910.
- (13) Tu, K. N.; Gösele, U. *Appl. Phys. Lett.* **2005**, *86*, 093111.

JA0646038